JOURNAL OF MATERIALS PROCESSING TECHNOLOGY 206 (2008) 167–179

journal homepage: www.elsevier.com/locate/jmatprotec

Experimental investigations of cutting parameters influence on cutting forces and surface roughness in finish hard turning of MDN250 steel

D.I. Lalwani, N.K. Mehta, P.K. Jain*

Department of Mechanical & Industrial Engineering, Indian Institute of Technology Roorkee, Roorkee, Uttarakhand 247667, India

ARTICLE INFO

Article history:
Received 20 August 2007
Received in revised form
31 October 2007
Accepted 4 December 2007

Keywords:
Finish hard turning
Maraging steel
Cutting forces
Surface roughness

ABSTRACT

In the present study, an attempt has been made to investigate the effect of cutting parameters (cutting speed, feed rate and depth of cut) on cutting forces (feed force, thrust force and cutting force) and surface roughness in finish hard turning of MDN250 steel (equivalent to 18Ni(250) maraging steel) using coated ceramic tool. The machining experiments were conducted based on response surface methodology (RSM) and sequential approach using face centered central composite design. The results show that cutting forces and surface roughness do not vary much with experimental cutting speed in the range of 55–93 m/min. A linear model best fits the variation of cutting forces with feed rate and depth of cut. Depth of cut is the dominant contributor to the feed force, accounting for 89.05% of the feed force whereas feed rate accounts for 6.61% of the feed force. In the thrust force, feed rate and depth of cut contribute 46.71% and 49.59%, respectively. In the cutting force, feed rate and depth of cut contribute 52.60% and 41.63% respectively, plus interaction effect between feed rate and depth of cut provides secondary contribution of 3.85%. A non-linear quadratic model best describes the variation of surface roughness with major contribution of feed rate and secondary contributions of interaction effect between feed rate and depth of cut, second-order (quadratic) effect of feed rate and interaction effect between speed and depth of cut. The suggested models of cutting forces and surface roughness adequately map within the limits of the cutting parameters considered.

1. Introduction

Industries around the world constantly strive for lower cost solutions with reduced lead time and better surface quality in order to maintain their competitiveness. Traditionally, most ferrous metal parts are rough turned, heat-treated and finished by grinding. In recent years, hard turning which uses a single point cutting tool has replaced grinding to some extent for such applications.

Finish hard turning is an emerging machining process which enables manufacturers to machine hardened materials having hardness greater than 45 HRC using a single point polycrystalline cubic boron nitride (PCBN commonly known as CBN) or ceramic cutting tool without any aid of cutting fluid on a rigid lathe or turning center (Narutaki et al., 1979; Hodgson et al., 1981; König et al., 1984; Tönshoff et al., 2000). This process has been developed as an alternative to the grinding process in a bid to reduce the number of setup changes, product cost

* *Corresponding author.*
E-mail addresses: dil@med.svnit.ac.in (D.I. Lalwani), mehtafme@iitr.ernet.in (N.K. Mehta), pjainfme@iitr.ernet.in (P.K. Jain).
0924-0136/$ – see front matter © 2007 Elsevier B.V. All rights reserved.
doi:10.1016/j.jmatprotec.2007.12.018

and lead time without compromising on surface quality to maintain competitiveness (Narutaki et al., 1979; Hodgson et al., 1981; König et al., 1984; Tönshoff et al., 2000).

For successful implementation of hard turning, selection of suitable cutting parameters for a given cutting tool; workpiece material and machine tool are important steps. Study of cutting forces is critically important in turning operations (Shaw, 1984) because cutting forces correlate strongly with cutting performance such as surface accuracy, tool wear, tool breakage, cutting temperature, self-excited and forced vibrations, etc. The resultant cutting force is generally resolved into three components, namely feed force (Fx), thrust force (Fy) and cutting force (Fz).

Finish hard turning differs from conventional turning of softer materials in several key ways. Because the material is harder, specific cutting forces (force per unit chip cross-section area) are larger than in conventional turning. Studies carried out by Tönshoff and Chryssolouris (1981) showed that specific cutting force when turning a 50CrMo4 steel (55 HRC) with CBN was 30% higher than while turning the same material in annealed condition. Similarly, König et al. (1984) found that cutting force was 50% larger and feed and thrust forces were 100% larger when turning a 100CrMo7 ball bearing steel of hardness 63 HRC as compared to turning the same material having hardness 32 HRC. Thrust force is larger than cutting force in finish hard turning as depth of cut and feed rate are very small compared to nose radius of the tool, which does the bulk of cutting (König et al., 1984; Kishawy and Elbestawi, 1999; Lin and Chen, 1995). Cutting tools used for hard turning are typically prepared with chamfered and/or honed edges to provide a stronger edge that is less prone to premature fracture. Cutting with a chamfered or honed edge gives a large negative effective rake angle, while neutral or positive rake angles are typical in conventional machining. The large negative rake angle yields increased cutting forces compared to machining with positive rake tools and also induce larger compressive loads on the machined surface and generate higher temperatures in the cutting zone. With large nose radius, small feed rate, small depth of cut and a large negative rake angle, ploughing effect (rubbing effect) can prevail and material side flow can also be observed as the result of the ploughing effect (Kishawy and Elbestawi, 1999; Huang and Liang, 2003). In addition, when undeformed chip thickness is extremely small and less than a critical value, the ploughing effect makes up a significant portion of the total cutting forces. Generally, this critical undeformed chip thickness is defined by tool nose radius, machine tool system stiffness and negative rake angle and needs to be carefully considered under these cutting configurations (Huang and Liang, 2003).

Yen et al. (2004) studied the effects of edge preparation of the cutting tool (round/hone edge and T-land/chamfer edge) on cutting forces using finite element analysis in orthogonal machining. Jawahir et al. (1992) carried out experimental studies on finish turning of low and medium carbon steel (AISI 1018 and 1045) with cermet tool for investigating machinability parameters such as chip breakability, surface roughness and specific cutting pressure. They proposed that a "total machinability" criterion can be formulated to represent the "cutting tool–work material–machine tool" system. Finite element modeling of forces and temperature in orthogonal machining of hardened AISI H13 (52 HRC) with CBN tool was carried out by Ng et al. (1999) and it was found that FE model underestimated the magnitude of cutting force due to limited data on the sensitivity of the workpiece material to strain hardening and the strain rate sensitivity at elevated temperature and oversimplification of the frictional conditions at the tool/chip interface. Benga and Abrao (2003) investigated the effect of speed and feed rate on surface roughness and tool life using three-level factorial design (3^2) on machining of hardened 100Cr6 bearing steel (62–64 HRC) using ceramic and CBN tools. They found that feed rate is the most significant factor affecting surface finish and cutting speed has very little influence on surface finish for both ceramic and CBN cutting tool. El-Wardany et al. (2000) investigated experimentally the effect of cutting parameters and tool wear on chip morphology and surface integrity during high-speed machining of D2 tool steel (60–62 HRC) using CBN tool. Özel et al. (2005) used a four-factor two-level factorial design (2^4) with 16 replications to determine the effects of the cutting tool edge geometry, workpiece hardness, feed rate and cutting speed on surface roughness and resultant forces in finish hard turning of AISI H13 steel using CBN tools. Further, Özel and Karpat (2005) developed predictive model of surface roughness and tool wear in hard turning using regression and neural network for AISI H13 steel using CBN tools. They considered work material hardness, CBN content in tool material, edge radius of the CBN cutting tool, cutting speed, feed rate and cutting time as independent parameters. Fang and Safi-Jahanshaki (1997) suggested linear and exponential empirical models for surface roughness as functions of cutting speed, feed rate and depth of cut. Feng and Wang (2002) developed an empirical model for surface roughness using two-level fractional factorial design (2^{5-1}) with three replicates considering workpiece hardness, feed rate, cutting tool point angle, depth of cut, cutting speed and cutting time as independent parameters using non-linear analysis. Thiele and Melkote (1999) used three-level factorial design to determine the effect of workpiece hardness, cutting edge geometry (edge radius and chamfer) on surface roughness and cutting forces in finish hard turning of AISI 52100 steel using CBN tools. The effect of tool material (Ceramic and CBN) and cutting parameters (speed, feed rate and depth of cut) on surface roughness was studied by Darwish (2000) using two-level factorial designs (2^3). He further demonstrated a favorable effect for ceramic inserts on surface roughness when compared with CBN inserts at both the high and low feed rates. The Taguchi method for optimizing the cutting parameters in turning operations was used by Yang and Kopač (Yang and Tarng, 1998; Kopač et al., 2002). Chen (2000) studied the cutting force and surface finish during machining of medium hardened steel (45–55 HRC) using CBN tool and concluded that thrust force was the largest among the three cutting force components. Recently, Arsecularatne et al. (2006) studied the machining of AISI D2 steel (62 HRC) with PCBN tools using three levels of speed and feed rate for studying tool life and cutting forces. They found that the relation between forces and cutting conditions (speeds and feeds for a constant depth of cut) was represented by power function-type equations (force = $A \times V^{a1} \times f^{a2}$, where A, $a1$, $a2$ are constants). Further, they stated that 70 m/min speed is

more suitable in machining selected tool/work material combination for highest acceptable value of tool life and volume of material removal.

Most of the experimental investigations on hard turning have been conducted using two-level factorial design (2^k) for studying influence of cutting parameters on cutting forces and surface roughness. In two-level factorial design, one can identify and model linear relationships only. For studying the nonlinearity present in the output characteristics at least three levels of each factor are required (i.e. three-level factorial design, 3^k). A central composite design which requires fewer experiments than alternative 3^k design is usually better. Again, sequential experimental approach in central composite design can be used to reduce the number of experiments required. Keeping the foregoing in mind, the present work is focused on investigations of cutting forces and surface roughness as a function of cutting parameters in finish hard turning using sequential approach in central composite design. The study was conducted on MDN250 steel (50 HRC) using coated ceramic tool.

2. Experimental details

The details of experimental conditions, instrumentations and measurements and the procedure adopted for the study are described in this section.

2.1. Workpiece material

MDN250 steel (equivalent to 18Ni(250) maraging steel) is a special class of high-strength steel which differs from conventional steels in the way that they are hardened by metallurgical reaction that does not involve carbon. Maraging steels (Rohrbach and Schmidt, 1990) are strengthened by the precipitation of intermetallic compound at temperatures of about 480 °C (900 °F). The distinguishing feature of this steel is superior toughness compared to other hardened steels. These steels typically have very high nickel, cobalt and molybdenum contents, small amounts of titanium and very low carbon contents. Carbon, in fact, is an impurity in these steels and is kept as low as commercially feasible in order to minimize the formation of titanium carbide (TiC), which can adversely affect strength, ductility and toughness. The nomenclature that has become established for these steels is nominal yield strength (ksi units) in parentheses. Thus, for an example, 18Ni(250) steel is normally age hardened to a yield strength of 1725 MPa (250 ksi). The most widely used and commonly available grades are 18Ni(200), 18Ni(250) and 18Ni(300). Maraging steels have been used in a wide variety of applications, including missile cases, aircraft forging, structural parts, cannon recoil, springs, bellaville springs, bearings, transmission shafts, fan shafts in commercial jet engines, couplings, hydraulic hoses, bolts, punches and dies (Rohrbach and Schmidt, 1990; Gupta et al., 1996).

Table 1 – Chemical composition of MDN250 steel (%)

C	0.005
Mn	0.02
Si	0.03
S	0.0032
P	0.005
Cr	0.03
Ni	17.97
Mo	4.93
Co	8.04
Ti	0.43
Al	0.09
Fe	Bal

Table 2 – Mechanical properties of MDN250 steel

0.2% PS (MPa)	1828
UTS (MPa)	1869
% Elongation	12
% Reduction in Area	61

Hard turning of bearing steel, tool steel, alloy steel, etc., was widely studied, but now there is an increasing interest in machining of MDN250 steel. Little work has been published on hard turning of MDN250 steel to the best of the knowledge of the authors. The MDN250 steel selected for the study has been provided by Mishra Dhatu Nigam Limited, Hyderabad (India).

Bars of MDN250 steel, 20 mm in diameter and 250 mm in length were used in the study. They were heat-treated at 485 °C for 3.5 h and then air-cooled. The hardness after heat treatment was obtained as 50.0 ± 0.5 HRC. The chemical compositions and mechanical properties of MDN250 steel as received are given in Tables 1 and 2, respectively.

2.2. Cutting tool

Coated ceramic inserts TNMA160408S01525 (Sandvik, Grade CC6050) were used in the experimental work with double clamp-type MTJNR 2525M16 (Mitsubishi Material Co.) tool holder. The edge preparation provided on the insert includes chamfered (25° × 0.15 mm) and honed edges both as illustrated in Fig. 1. Chamfer width was measured with Toolmaker's microscope with three replications and was found to have

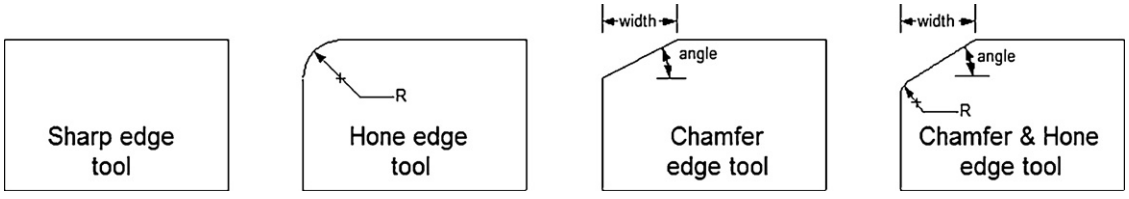

Fig. 1 – Type of edge preparations used in CBN and ceramic cutting tools in hard turning.

0.16 ± 0.01 mm. The tool angles are as follows:

back rake angle = −6°, side rake angle
= −6°, principal cutting edge angle
= 93°, end cutting edge angle = 27°.

2.3. Machine tool

Rigid, high power precision NH22 (HMT, India) lathe equipped with specially designed experimental setup was used for experimentation. For increasing rigidity of machining system, workpiece material was held between chuck (three jaws) and tailstock (revolving center) and the tool overhang was kept at the minimum possible value of 20 mm. Ceramic inserts were also examined using a large Toolmaker's microscope to measure flank wear width and to detect undesirable features on the edge of the cutting tool. The cutting was continued until the tool flank wear was reached 0.2 mm.

2.4. Cutting conditions

Lin and Chen (1995) studied cutting forces and surface roughness as function of cutting speed (44.5, 83, 144.5 m/min), feed rate (0.039, 0.104, 0.210, 0.216 mm/rev) and depth of cut (0.2 mm) for 64 HRC hardened bearing steel. Chen (2000) also, studied the cutting forces and surface roughness for 45–55 HRC steel using CBN tool for the cutting speed (56–182 m/min), feed rate (0.08–0.31 mm/rev) and depth of cut (0.025–0.1 mm).

Based on (Lin and Chen, 1995; Chen, 2000) and tool manufacturer recommendations, pilot tests were conducted and feasible range of cutting parameters for a given cutting tool–workpiece system were selected as follows (Table 3).

2.5. Cutting forces measurements

It was necessary to design a fixture to mount a force dynamometer on the lathe in such a way that tool tip will lie at the exact center of lathe axis. The cutting forces were measured using Kistler® piezoelectric dynamometer (model 9257B) mounted on specially designed fixture. Kistler® tool holder (model: 9403) was used for holding the 25 × 25 shank size cutting tool. The charge generated at the dynamometer was amplified using three-charge amplifier (Mescon Instruments, India, Model: CA 190). The input sensitivities of the three-charge amplifiers were set corresponding to the output sensitivity of the force dynamometer in the *x*, y and z directions. The output sensitivity was set for 100 N/V for cutting force (Fz), and 50 N/V for feed force (Fx) and thrust force (Fy) on the respective charge amplifier. The amplified signal was acquired and sampled using USB data acquisition system (Advantech make, Model 4711) and stored in computer using LabVIEW software for further analysis. The sampling frequency of data was kept at 1000 samples/s per channel and the average value of steady-state force was used in the analysis.

2.6. Surface roughness measurements

The measurements of average surface roughness (Ra) were made on the Veeco WYKO NT1100 surface profilometer with WYKO Vision32 V2.303 software using vertical scanning interferometry (VSI) mode at 10× magnification, full resolution and 1× scan speed. The cylinder and tilt were removed after taking measurements. Removing the cylinder will cause a cylindrical object to appear flat, so surface features can be observed instead of the dominant cylindrical shape, thereby removing any tilt between the system and the sample (Lamb and Zecchino, 1999). Three measurements of surface roughness were taken at different locations and the average value was used in the analysis.

2.7. Response surface methodology

Response surface methodology (RSM) is a collection of mathematical and statistical techniques that are useful for the modeling and analysis of problems in which a response of interest is influenced by several variables and the objective is to optimize this response (Montgomery, 2001).

i. Factorial/cube points (2^3) with or without replication, plus 2–4 center points.
ii. Axial/star points with or without replication (2 × number of factors), plus 2–4 center points.

The number of experiments in step 2 is to be carried out only if curvature (nonlinearity) is observed after doing statistical analysis in step 1.

2.8. Experimental plan procedure

Twenty experimental runs composed of eight factorial points with replication (16 runs), plus four center points were carried out in block 1 and 6 axial, plus 2 center points (8 runs) were carried out in block 2. Table 4 shows complete design matrix with responses (cutting forces and surface finish). In design matrix, the coded variables were arranged as follows: A: cutting speed (*V*), B: feed rate (*f*) and C: depth of cut (*d*). Fx, Fy, Fz and Ra are the responses representing feed force, thrust force, cutting force and surface roughness, respectively. The exper-

Table 3 – Cutting parameters and their levels

Factor	Unit	Low level (−1)	Center level (0)	High level (1)
A: Speed	m/min	55	74	93
B: Feed rate	mm/rev	0.04	0.08	0.12
C: Depth of cut	mm	0.1	0.15	0.2

Table 4 – Design matrix with responses (cutting forces and surface roughness)

Std	Run	Block	Type	A:*V* (m/min)	B:*f* (mm/rev)	C:*d* (mm)	A:*V* (m/min)	B:*f* (mm/rev)	C:*d* (mm)	Fx (N)	Fy (N)	Fz (N)	Ra (nm)
1	8	1	Fact	−1	−1	−1	55	0.04	0.1	17.93	54.59	24.73	438.33
2	1	1	Fact	−1	−1	−1	55	0.04	0.1	18.92	56.88	26.93	431.30
3	2	1	Fact	1	−1	−1	93	0.04	0.1	15.34	52.56	21.29	560.21
4	14	1	Fact	1	−1	−1	93	0.04	0.1	15.90	49.72	23.20	567.02
5	6	1	Fact	−1	1	−1	55	0.12	0.1	24.06	85.94	47.52	722.63
6	12	1	Fact	−1	1	−1	55	0.12	0.1	24.40	85.23	48.48	723.55
7	13	1	Fact	1	1	−1	93	0.12	0.1	23.27	84.20	45.79	745.65
8	5	1	Fact	1	1	−1	93	0.12	0.1	20.37	78.49	45.10	725.18
9	7	1	Fact	−1	−1	1	55	0.04	0.2	42.20	87.63	44.59	429.38
10	3	1	Fact	−1	−1	1	55	0.04	0.2	37.40	79.32	41.34	459.27
11	19	1	Fact	1	−1	1	93	0.04	0.2	43.01	88.51	43.07	387.77
12	20	1	Fact	1	−1	1	93	0.04	0.2	40.43	82.48	44.18	434.48
13	11	1	Fact	−1	1	1	55	0.12	0.2	45.08	116.40	78.62	836.55
14	18	1	Fact	−1	1	1	55	0.12	0.2	47.68	126.76	88.63	849.70
15	9	1	Fact	1	1	1	93	0.12	0.2	51.87	125.10	83.17	820.37
16	15	1	Fact	1	1	1	93	0.12	0.2	47.53	118.20	80.79	853.56
17	17	1	Center	0	0	0	74	0.08	0.15	25.85	77.32	43.30	566.22
18	10	1	Center	0	0	0	74	0.08	0.15	32.42	87.13	50.41	580.79
19	4	1	Center	0	0	0	74	0.08	0.15	29.93	83.86	48.04	568.24
20	16	1	Center	0	0	0	74	0.08	0.15	35.20	91.62	53.33	544.21
21	25	2	Axial	−1	0	0	55	0.08	0.15				482.28
22	28	2	Axial	1	0	0	93	0.08	0.15				467.39
23	23	2	Axial	0	−1	0	74	0.04	0.15				364.21
24	24	2	Axial	0	1	0	74	0.12	0.15				710.37
25	21	2	Axial	0	0	−1	74	0.08	0.1				408.61
26	27	2	Axial	0	0	1	74	0.08	0.2				416.69
27	22	2	Center	0	0	0	74	0.08	0.15				565.67
28	26	2	Center	0	0	0	74	0.08	0.15				555.24

iments were conducted randomly as shown in design matrix ('runs' column in Table 4). The design matrix also, shows the factorial points, center points and axial points with coded and actual values.

3. Results and discussion

Table 4 shows all values of cutting forces and surface roughness. The surface roughness was obtained in the range of 364.21 nm to 853.56 nm. The feed force, thrust force and cutting force were obtained in the range of 15.34–51.87 N, 49.72–126.76 N and 21.29–88.63 N, respectively. Furthermore, thrust force is about 1.5–2.5 higher than cutting force. König et al. (1984) reported that thrust force is about twice that of cutting force in hard turning. The thrust force is larger than cutting force in hard turning is also reported by König et al. (1984), Kishawy and Elbestawi (1999), Lin and Chen (1995), Chen (2000). The increase in thrust force is due to ploughing effect that prevails under the conditions of small feed rate, small depth of cut compared to nose radius and a large negative rake angle. Lin and Chen (1995) also, observed that when depth of cut is increased (i.e. cutting does not take place at nose radius), the cutting force was larger than the thrust force.

Fig. 2 shows relation between cutting forces and speed for different feed rates at a depth of cut of 0.1 mm. The cutting forces are almost constant with respect to cutting speed.

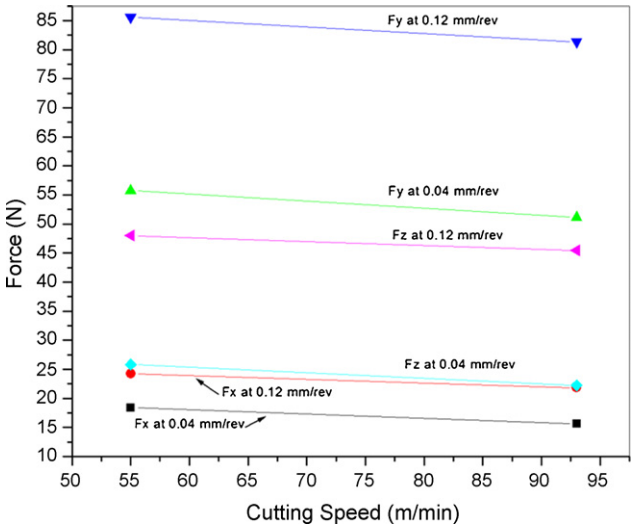

Fig. 2 – Cutting forces vs. cutting speed at various feed rate and constant depth of cut 0.1 mm.

This observation agrees well with results reported by previous researchers (Huang and Liang, 2005; Chou and Evans, 1999).

Furthermore, the results were analyzed in Design Expert V6 software. The results of the block 1 experiments in the form of

Table 5 – ANOVA (partial sum of square) for feed force (Fx)

Source	Sum of squares	d.f.	Mean square	F-value	Prob > F	% Contribution	Remark
Model	2583.262	7	369.0374	50.90429	<0.0001		Significant
A: Cutting speed	0.000106	1	0.000106	1.47E-05	0.9970	3.98E-06	
B: Feed rate	176.4508	1	176.4508	24.33927	0.0004	6.611304	Significant
C: Depth of cut	2376.773	1	2376.773	327.8474	<0.0001	89.05356	Significant
AB	0.805416	1	0.805416	0.111097	0.7452	0.030178	
AC	27.32881	1	27.32881	3.769682	0.0782	1.023963	
BC	1.649759	1	1.649759	0.227564	0.6427	0.061814	
ABC	0.253758	1	0.253758	0.035003	0.8550	0.009508	
Curvature	5.917788	1	5.917788	0.816288	0.3856	0.221729	Not significant
Pure error	79.74597	11	7.249633				
Cor total	2668.926	19					

Table 6 – ANOVA (partial sum of square) for feed force (Fx) after removing insignificant terms

Source	Sum of squares	d.f.	Mean square	F-value	Prob > F	% Contribution	Remark
Model	2553.224	2	1276.612	186.0547	<0.0001		
B: Feed rate	176.4508	1	176.4508	25.71611	0.0001	6.611304	
C: Depth of cut	2376.773	1	2376.773	346.3933	<0.0001	89.05356	
Curvature	5.917788	1	5.917788	0.862464	0.3668	0.221729	Not significant
Residual	109.7838	16	6.861488				
Lack of fit	30.03785	5	6.00757	0.828672	0.5551		Not significant
Pure error	79.74597	11	7.249633				
Cor total	2668.926	19					
S.D.	2.619444		R^2	0.958775			
Mean	31.93991		R^2_{Adj}	0.953621			
C.V. (%)	8.201164		R^2_{Pred}	0.933043			

Table 7 – ANOVA (partial sum of square) for thrust force (Fy) after removing insignificant terms

Source	Sum of squares	d.f.	Mean square	F-value	Prob > F	% Contribution	Remark
Model	9299.054	2	4649.527	209.096	<0.0001		Significant
B: Feed rate	4510.702	1	4510.702	202.8529	<0.0001	46.71041	
C: Depth of cut	4788.352	1	4788.352	215.3392	<0.0001	49.5856	
Curvature	1.903824	1	1.903824	0.085618	0.7736	0.019715	Not significant
Residual	355.7812	16	22.23632				
Lack of fit	93.62839	5	18.72568	0.785734	0.5809		Not significant
Pure error	262.1528	11	23.83207				
Cor total	9656.739	19					
S.D.	4.715541		R^2	0.96315			
Mean	85.59712		R^2_{Adj}	0.958544			
C.V. (%)	5.508994		R^2_{Pred}	0.941231			

analysis of variance (ANOVA) are presented. An ANOVA summary table is commonly used to summarize the test of the regression model, test of the significance factors and their interaction and lack-of-fit test. If the value of 'Prob > F' in ANOVA table is less than 0.05 then the model, the factors, interaction of factors and curvature are said to be significant. Finally, % contribution column is added in ANOVA summary table and it often serves as a rough but an effective indicator of the relative importance of each model term (Montgomery, 2001).

3.1. *Feed force (Fx)*

Table 5 shows that the model is significant and feed rate (B) and depth of cut (C) are only the significant factors (terms) in the model. All other terms are insignificant. The percentage contribution of factors, their interaction and curvature is also shown in Table 5. By selecting the significant terms, the resulting ANOVA table for reduced model is shown in Table 6. Table 6 shows that the model is still significant and curvature is insignificant which indicates that model is linear. The lack-of-fit is insignificant thereby indicates that the model fits well with the experimental data. Depth of cut is the dominant contributor to the feed force, accounting for 89.05% of total variability whereas feed rate accounts for 6.61% of the total variability. This indicates that feed rate has little influence on feed force and it agrees with the results of Özel et al. (2005).

In finish hard turning as depth of cut (0.1–0.2 mm) is very small compared to nose radius of tool (0.8 mm) and cutting takes place at nose radius only. This results in varying principal cutting edge angle along the nose radius of the tool and the maximum principal cutting edge angle can be obtained as $K_r = \cos^{-1}((r_\varepsilon - d)/r_\varepsilon)$ (Shaw, 1984; Chen, 2000; Oxley, 1989), where r_ε is nose radius and 'd' is depth of cut. To illustrate, for a tool of nose radius, $r_\varepsilon = 0.8$ mm, as the depth of cut is increased from 0.1 to 0.2 mm, K_r increases from 28.96° to 41.41°. This explains the predominant role of depth of cut in the feed force (Chen, 2000).

The various R^2 statistics (i.e. R^2, adjusted R^2 (R^2_{Adj}) and predicted R^2 (R^2_{Pred})) of the feed force are given in Table 6. The value of $R^2 = 0.9588$ for feed force indicates that 95.88% of the total variations are explained by the model. The adjusted R^2 is a statistic that is adjusted for the "size" of the model; that is, the number of factors (terms). The value of the $R^2_{Adj} = 0.9536$ indicates that 95.36% of the total variability is explained by the model after considering the significant factors. $R^2_{Pred} = 0.9330$ is in good agreement with the R^2_{Adj} and shows that the model would be expected to explain 93.30% of the variability in new data (Montgomery, 2001). 'C.V.' stands for the coefficient of variation of the model and it is the error expressed as a percentage of the mean ((S.D./Mean) × 100). Lower value of

Table 8 – ANOVA (partial sum of square) for cutting force (Fz) after removing insignificant terms

Source	Sum of squares	d.f.	Mean square	F-value	Prob > F	% Contribution	Remark
Model	7213.359	3	2404.453	257.1021	<0.0001		Significant
B: Feed rate	3868.239	1	3868.239	413.6211	<0.0001	52.59853	
C: Depth of cut	3062.147	1	3062.147	327.4277	<0.0001	41.63766	
BC	282.973	1	282.973	30.25759	<0.0001	3.847736	
Curvature	0.63087	1	0.63087	0.067457	0.7986	0.008578	Not significant
Residual	140.282	15	9.352132				
Lack of fit	22.53732	4	5.634329	0.526373	0.7189		Not significant
Pure error	117.7447	11	10.70406				
Cor total	7354.272	19					
S.D.	3.058126		R^2	0.980923			
Mean	49.1256		R^2_{Adj}	0.977108			
C.V. (%)	6.225115		R^2_{Pred}	0.966089			

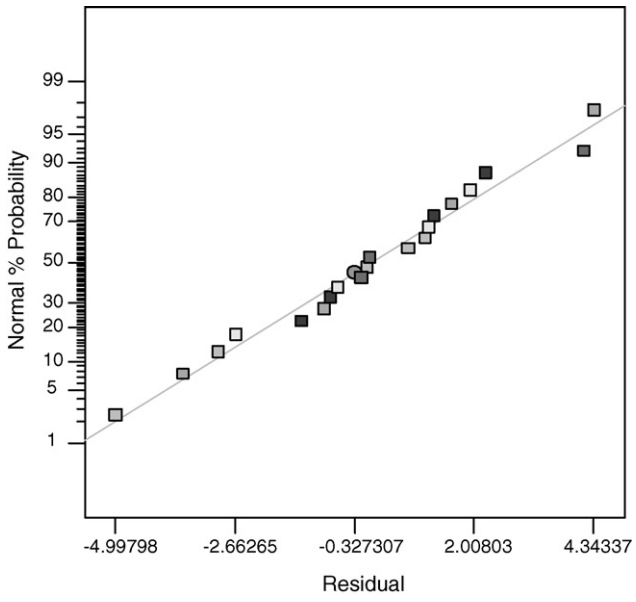

Fig. 3 – Normal probability plot of residuals for feed force (Fx) data.

the coefficient of variation (C.V. = 8.20%) indicates improved precision and reliability of the conducted experiments. As curvature (nonlinearitly) is not present in the model, additional experiments mentioned in block 2 of Table 4 are not required to be performed. This is the main advantage of sequential approach in face centered central composite design.

The same procedure was applied on thrust force (Fy) and cutting force (Fz) and resulting ANOVA with R^2 statistics for reduced models (considering only the significant terms) are shown in Tables 7 and 8, respectively.

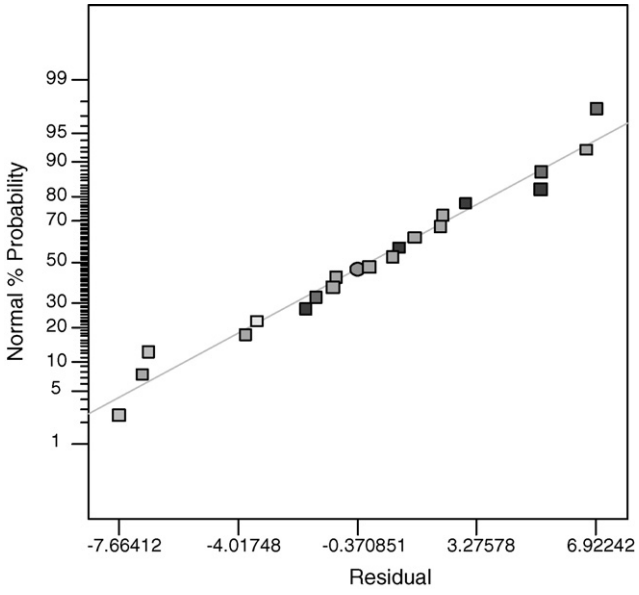

Fig. 4 – Normal probability plot of residuals for thrust force (Fy) data.

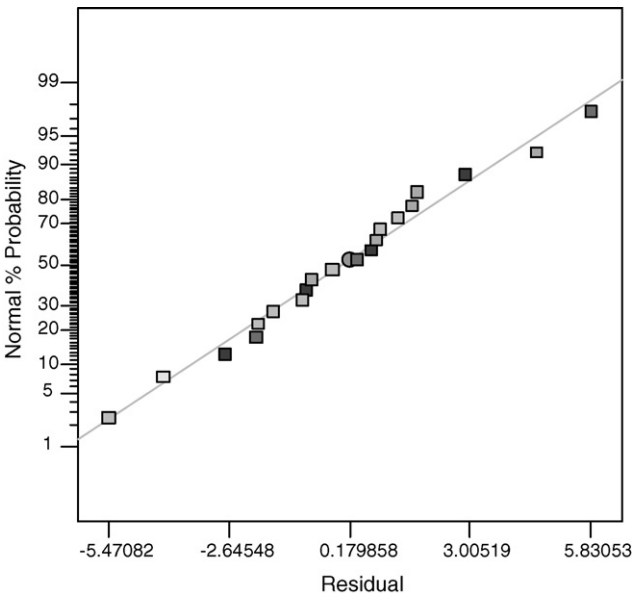

Fig. 5 – Normal probability plot of residuals for cutting force (Fz) data.

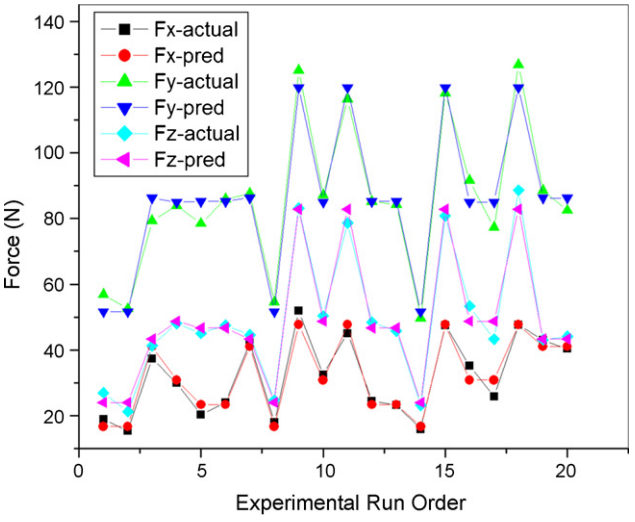

Fig. 6 – Actual vs. predicted values of cutting forces.

3.2. *Thrust force (Fy)*

For thrust force (Table 7), the feed rate and depth of cut contribute 46.71% and 49.59% in the total variability of model, respectively. Curvature (nonlinearity) is not significant which again indicates that the model is linear. The significance of feed rate for the thrust force agrees with results of Özel et al. (2005).

3.3. *Cutting force (Fz)*

For cutting force (Table 8), the feed rate and depth of cut contribute 52.60% and 41.63% in the total variability of model, respectively. Additionally, it is observed that the interaction

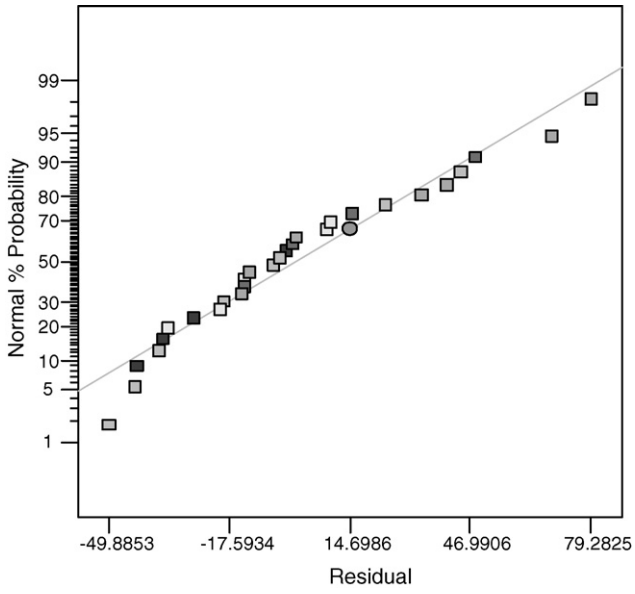

Fig. 7 – Normal probability plot of residuals for surface roughness (Ra) data.

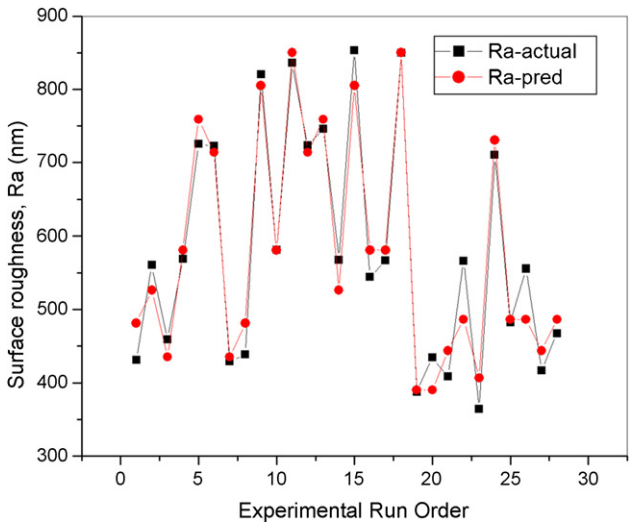

Fig. 8 – Actual vs. predicted values of surface roughness (Ra).

between feed rate and depth of cut provides secondary contributions (3.85%) to the cutting force and curvature is not significant. Thiele and Melkote (1999) also, reported that feed rate provides the main contribution to cutting force.

After removing the insignificant factors, the response surface equations for cutting forces are obtained in the actual values as follows:

$$\text{Fx} = -10.994 + 83.02174 \times \text{Feed rate} + 243.7608 \times \text{Depth of cut} \pm \varepsilon \quad (1)$$

$$\text{Fy} = 0.272064 + 419.761 \times \text{Feed rate} + 345.9896 \times \text{Depth of cut} \pm \varepsilon \quad (2)$$

$$\text{Fz} = 1.847022 + 73.31105 \times \text{Feed rate} + 108.4653 \times \text{Depth of cut} + 2102.725 \times \text{Feed rate} \times \text{Depth of cut} \pm \varepsilon \quad (3)$$

The normal probability plot of the residuals (i.e. error = predicted value from model − actual value) for feed force, thrust force and cutting force is shown in Figs. 3–5, respectively. Figs. 3–5 reveal that the residuals lie reasonably close to a straight line, giving support that terms mentioned in the model are the only significant (Montgomery, 2001). Fig. 6 also, shows the predicted values of cutting forces from response surface equations and the actual (experimental) values.

3.4. *Surface roughness*

Table 9 shows that cutting speed (A), feed rate (B) and depth of cut (C); two-level interaction effect of cutting speed and feed

Table 9 – ANOVA (partial sum of square) for surface roughness (Ra) after removing insignificant terms (first 20 experiments)

Source	Sum of squares	d.f.	Mean square	*F*-value	Prob > *F*	% Contribution	Remark
Model	465277.5	7	66468.21	233.8738	<0.0001		Significant
A: Cutting speed	2589.114	1	2589.114	9.110005	0.0117	0.539828	
B: Feed rate	412624.2	1	412624.2	1451.852	<0.0001	86.0318	
C: Depth of cut	1544.621	1	1544.621	5.434874	0.0398	0.322052	
AB	1999.729	1	1999.729	7.036209	0.0225	0.416942	
AC	8143.558	1	8143.558	28.65377	0.0002	1.697925	
BC	33227.21	1	33227.21	116.9126	<0.0001	6.927846	
ABC	5149.019	1	5149.019	18.11724	0.0014	1.073566	
Curvature	11214.53	1	11214.53	39.45924	<0.0001	2.33822	Significant
Pure error	3126.26	11	284.2055				
Cor total	479618.3	19					
S.D.	16.8584		R^2	0.993326			
Mean	612.2193		R^2_{Adj}	0.989078			
C.V. (%)	2.753653		R^2_{Pred}	0.97714			

Table 10 – Model summary statistics of surface roughness

Model	S.D.	R^2	R^2_{Adj}	R^2_{Pred}	Remarks
Linear	62.72233	0.840202	0.819359	0.757984	
2FI	48.53533	0.916796	0.891834	0.861965	
Quadratic	38.4921	0.955517	0.931968	0.892634	Suggested
Cubic	38.20868	0.966483	0.932966	−3.27636	Aliased

Table 11 – ANOVA (partial sum of square) for surface roughness (Ra) with axial, plus center points after removing insignificant terms

Source	Sum of squares	d.f.	Mean square	F-value	Prob > F	Remarks
Block	76774.92	1	76774.92			
Model	529304.7	4	132326.2	78.81847	<0.0001	Significant
B: Feed rate	472261.3	1	472261.3	281.2967	<0.0001	
AC	8143.558	1	8143.558	4.850611	0.0384	
BC	33227.21	1	33227.21	19.79138	0.0002	
B^2	15672.62	1	15672.62	9.335203	0.0058	
Residual	36935.2	22	1678.873			
Lack of fit	33754.49	10	3375.449	12.73471	<0.0001	
Pure error	3180.709	12	265.059			
Cor total	643014.8	27				
S.D.	40.97405		R^2	0.934771		
Mean	579.1016		R^2_{Adj}	0.922911		
C.V. (%)	7.075451		R^2_{Pred}	0.902402		

rate (AB), cutting speed and depth of cut (AC), feed rate and depth of cut (BC) and three-level interaction effect of cutting speed, feed rate and depth of cut (ABC) all have significant effect on the surface roughness. But the effect of feed rate (B) is the most significant factor associated with surface roughness with 86.03% contribution to the model. This is anticipated as it is well known that for a given tool nose radius, the theoretical surface roughness ($Ra \cong f^2/(32 \times r_\varepsilon)$) is mainly a function of the feed rate (Shaw, 1984). All other terms provide secondary contribution to the surface roughness in the descending order of BC, AC, ABC, A, AB and C.

Table 9 also, shows that the curvature is significant and therefore, additional 8 experiments are further required to be carried out (6 axial + 2 center) to account for the nonlinearity present in the model. After augmenting the design with six axial points and two center points (Table 4, Block 2),

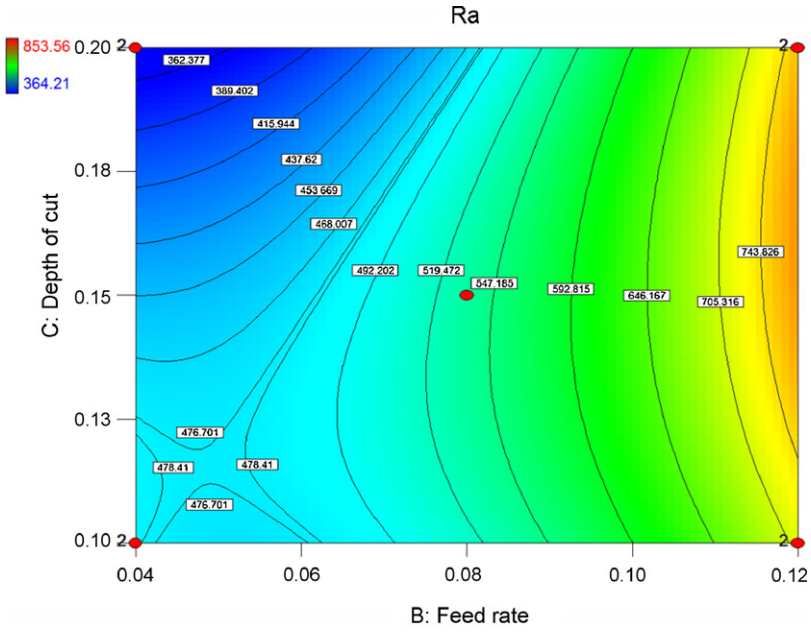

Fig. 9 – Surface roughness contour in feed rate and depth of cut plane at cutting speed of 93 m/min (●, design points).

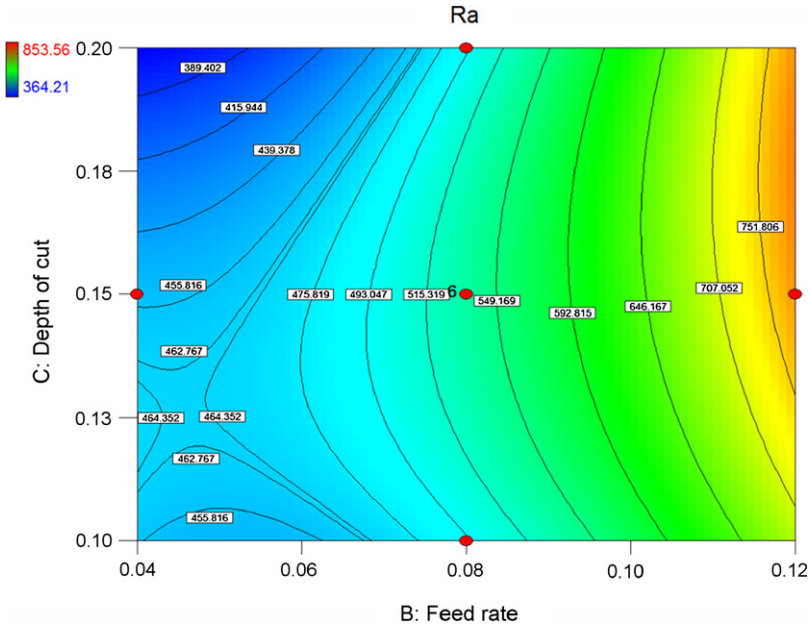

Fig. 10 – Surface roughness contour in feed rate and depth of cut plane at cutting speed of 74 m/min (●, design points).

summary statistics of model are shown in Table 10. Table 10 clearly shows that the quadratic model is the best suggested model for surface roughness with larger R^2 statistics value. The ANOVA analysis, after removing insignificant term for quadratic model of surface roughness is shown in Table 11. Results show that the feed rate is the most significant factor affecting the surface roughness. The interaction between feed rate and depth of cut (BC); quadratic effect of feed rate (B^2) and interaction between speed and depth of cut (AC) provide secondary contribution to surface roughness.

The effect of cutting speed as a main factor alone is not significant. This observation is in agreement with the findings of previous researchers (Benga and Abrao, 2003; El-Wardany et al., 2000; Oishi, 1995). However, it is pertinent to note that the interaction of cutting speed with depth of cut is significant which implies that as a secondary factor cutting speed affects surface roughness.

The final response surface equation for quadratic model of surface roughness is shown in coded values in equation 4. In this model a hierarchy is not followed which promotes an internal consistency in the model. It is suggested by Montgomery (2001) that hierarchy is not always a good idea and many models actually work better as prediction equations without including the insignificant factors that promote

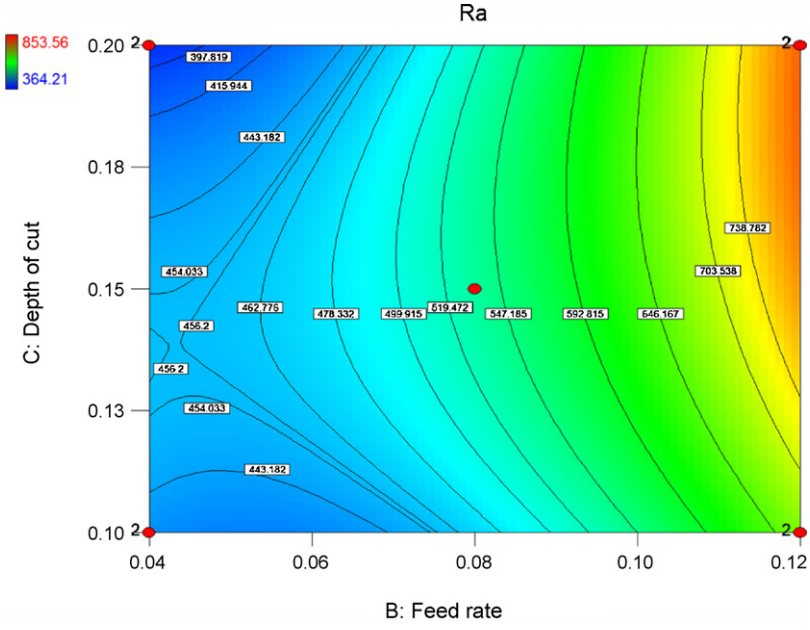

Fig. 11 – Surface roughness contour in feed rate and depth of cut plane at cutting speed of 55 m/min (●, design points).

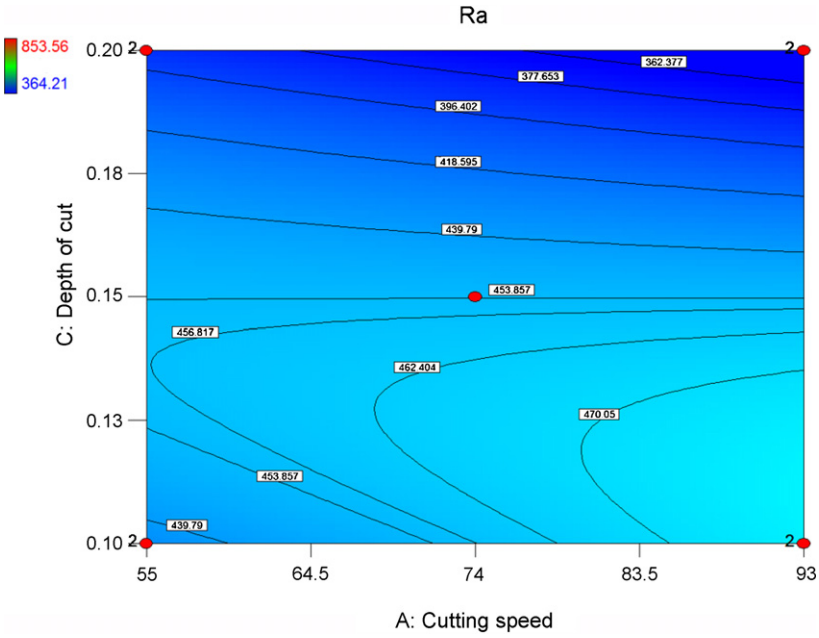

Fig. 12 – Surface roughness contour in cutting speed and depth of cut plane at feed rate of 0.04 mm/rev (●, design points).

hierarchy.

$$\text{Ra} = 523.9466 + 161.9776 \times \text{B} - 22.5604 \times \text{A} \times \text{C} + 45.57083 \times \text{B} \times \text{C} + 57.74599 \times \text{B}^2 \pm \varepsilon \quad (4)$$

The normal probability plot of the residuals surface roughness is shown in Fig. 7 which shows that the residuals lie reasonably close to a straight line, giving support that terms mentioned in the model are the only significant (Montgomery, 2001). The predicted values from the model and the actual values are shown in Fig. 8.

Since hard turning is sought to be used as a replacement of grinding, the major focus of research is to find cutting conditions for which desired surface roughness can be achieved. Hence, the contour plots of the surface roughness in feed rate-depth of cut plane at cutting speeds of 93, 74 and 53 m/min are shown in Figs. 9–11, respectively. The curvilinear profile is in agreement with quadratic model fitted. Figs. 9–11 clearly show that a good surface finish can be achieved for any level of cutting speed (i.e. 55, 74, 93 m/min), when feed rate is low (0.04 mm/rev) and depth of cut is high (0.2 mm). Based on the Figs. 9–11, Fig. 12 was prepared which shows contour plot of surface roughness in speed-depth of cut plane at a feed rate of 0.04 mm/rev. For getting required surface roughness what cutting parameters are to be selected can be best judge from Fig. 12.

4. Conclusions

This paper presents the findings of an experimental investigation of the effect of cutting speed, feed rate and depth of cut on the feed force, thrust force, cutting force and surface roughness in finish hard turning of MDN250 (50 HRC) steel using coated ceramic tool and following conclusions are drawn.

- Sequential approach in central composite design is beneficial as it saves number of experimentations required. This was observed in force analysis.
- Linear model is fitted for feed force, thrust force and cutting force whereas quadratic model is fitted for surface roughness.
- Cutting speed has no significant effect on cutting forces and surface roughness.
- Feed force model: the depth of cut is most significant factor with 89.05% contribution in the total variability of model whereas feed rate has a secondary contribution of 6.61% in the model.
- Thrust force model: the feed rate and depth of cut are significant factor with 46.71% and 49.59% contribution in the total variability of model, respectively.
- Cutting force model: the feed rate and depth of cut are the most significant factors affecting cutting force and account for 52.60% and 41.64% contribution in the total variability of model, respectively. The interaction between these two provides a secondary contribution of 3.85%.
- Surface roughness model: the feed rate provides primary contribution and influences most significantly on the surface roughness. The interaction between feed rate and depth of cut, quadratic effect of feed rate and interaction effect of speed and depth of cut provide secondary contribution to the model.
- Good surface roughness can be achieved when cutting speed and depth of cut are set nearer to their high level of the experimental range (93 m/min and 0.2 mm) and feed rate is at low level of the experimental range (0.04 mm/rev). This is borne by the fact that when cutting speed is increased from 55 to 93 m/min at a depth of cut = 0.2 mm and feed rate = 0.04 mm/rev, the surface roughness decreases from 0.397 to 0.352 μm (Eq. (4)) which amounts to an 11.33% reduction of the surface roughness value and is attributed

to the secondary effect of interaction between cutting speed and depth of cut.
- Contour plots can be used for selecting the cutting parameters for providing the given desired surface roughness.

Acknowledgements

The authors wish to thank Mr. K. Ramesh and Mr. I.S.N. Murthy of M/s Mishra Dhatu Nigam Ltd., Hydreabad, India, for providing help and support in procurement of the workpiece material MDN250 steel for research work.

REFERENCES

Arsecularatne, J.A., Zhang, L.C., Montross, C., Mathew, P., 2006. On machining of hardened AISI D2 steel with PCBN tools. J. Mater. Process. Technol. 171, 244–252.

Benga, G.C., Abrao, A.M., 2003. Turning of hardened 100Cr6 bearing steel with ceramic and PCBN cutting tools. J. Mater. Process. Technol. 143-144, 237–241.

Chen, W., 2000. Cutting forces and surface finish when machining medium hardness steel using CBN tools. Int. J. Mach. Tools Manuf. 40, 455–466.

Chou, Y.K., Evans, C.J., 1999. White layers and thermal modeling of hard turned surfaces. Int. J. Mach. Tools Manuf. 39, 1863–1881.

Darwish, S.M., 2000. The impact of the tool material and the cutting parameters on surface roughness of supermet 718 nickel superalloy. J. Mater. Process. Technol. 97, 10–18.

El-Wardany, T.I., Kishawy, H.A., Elbestawi, M.A., 2000. Surface integrity of die material in high speed hard machining. Part 1. Micrographical analysis. ASME Trans., JMSE 122, 620–631.

Fang, X.D., Safi-Jahanshaki, H., 1997. A new algorithm for developing a reference model for predicting surface roughness in finish machining of steels. Int. J. Prod. Res. 35 (1), 179–197.

Feng, C.X.J., Wang, X., 2002. Development of empirical models for surface roughness prediction in finish turning. Int. J. Adv. Manuf. Technol. 20, 348–356.

Gupta, B., Gopala, K.V., Yadav, J.S., 1996. Aerospace materials: With General Metallurgy for Engineers. S. Chand and Co. Ltd., New Delhi, India.

Hodgson, T., Trendler, P., Ravignani, G., 1981. Turning hardened tool steels with cubic boron nitride inserts. Ann. CIRP 30 (1), 63–66.

Huang, Y., Liang, S.Y., 2003. Force modeling in shallow cuts with larger negative rake angle and large nose radius tools—applications to hard turning. Int. J. Adv. Manuf. Technol. 22, 626–632.

Huang, Y., Liang, S.Y., 2005. Modeling of cutting forces under hard turning conditions considering tool wear effect. ASME J. Manuf. Sci. Eng. 127, 262–270.

Jawahir, I.S., Qureshi, N., Arsecularatne, J.A., 1992. On the interrelationships of some machinability parameters in finish turning with cermet chip forming tool inserts. Int. J. Mach. Tools Manuf. 32 (5), 709–723.

Kishawy, H.A., Elbestawi, M.A., 1999. Effects of process parameters on material side flow during hard turning. Int. J. Mach. Tools Manuf. 39, 1017–1030.

König, W., Komanduri, R., Tönshoff, H., Ackershott, G., 1984. Machining of hard materials. Ann. CIRP 33 (2), 417–428.

Kopač, J., Bahor, M., Soković, M., 2002. Optimal machining parameters for achieving the desired surface roughness in fine turning of cold pre-formed steel workpieces. Int. J. Mach. Tools Manuf. 42, 707–716.

Lamb, C., Zecchino, M., 1999. Wyko Surface Profilers Technical Reference Manual. Veeco Metrology Group, Arizona.

Lin, Z.-C., Chen, D.-Y., 1995. A study of cuttting with CBN tool. J. Mater. Process. Technol. 49, 149–164.

Montgomery, D.C., 2001. Design and Analysis of Experiments, 5th ed. John Wiley & Sons Inc.

Narutaki, N., Yamane, Y., Okushima, K., 1979. Tool wear and cutting temperature of CBN tool in machining of hardened steels. Ann. CIRP 28 (1), 23–28.

Ng, E.G., Aspinwall, D.K., Brazil, D., Monaghan, J., 1999. Modeling of temperature and forces when orthogonally machining hardened steel. Int. J. Mach. Tools Manuf. 39, 885–903.

Oishi, K., 1995. Built-up edge elimination in mirror cutting of hardened steel. ASME J. Eng. Ind. 117 (1), 62–66.

Oxley, P.L.B., 1989. The Mechanics of Machining: An Analytical Approach to Assessing Machinability. Ellis Horwood Ltd., West Sussex, England.

Özel, T., Karpat, Y., 2005. Predictive modeling of surface roughness and tool wear in hard turning using regression and neural networks. Int. J. Mach. Tools Manuf. 45, 467–479.

Özel, T., Hsu, T.-K., Zeren, E., 2005. Effects of cutting edge geometry, workpiece hardness, feed rate and cutting speed on surface roughness and forces in finish turning of hardened AISI H13 steel. Int. J. Adv. Manuf. Technol. 25, 262–269.

Rohrbach, K., Schmidt, M., 1990. Maraging steels. In: Abel, L.A., Kiepura, R.T., Thomas, P., Wheaton, N.D. (Eds.), Properties and Selection: Irons, Steels, and High-performance Alloys of ASM Handbook, Vol. I, 10th ed. ASM Int..

Shaw, M.C., 1984. Metal Cutting Principles. Oxford University Press, Oxford, NY.

Thiele, J.D., Melkote, S.N., 1999. Effect of cutting edge geometry and workpiece hardness on surface generation in the finish hard turning of AISI 52100 steel. J. Mater. Process. Technol. 94, 216–226.

Tönshoff, H.K., Chryssolouris, G., 1981. Einsatz kubischen boronitrids (cbn) beim drehen gehaerteter staehle. Werkstatt und Betrier 114 (1), 45–49.

Tönshoff, H.K., Arendt, C., Amor, R.B., 2000. Cutting hardened steel. Ann. CIRP 49 (2), 1–19.

Yang, W.H., Tarng, Y.S., 1998. Design optimization of cutting parameters for turning operations based on the Taguchi method. J. Mater. Process. Technol. 84, 122–129.

Yen, Y.-C., Jain, A., Altan, T., 2004. A finite element analysis of orthogonal machining using different tool edge geometries. J. Mater. Process. Technol. 146, 72–81.